Behavior of Acetonitrile Confined to Mesoporous Silica Gels As Studied by ^{129}Xe NMR: A Novel Method for Determining the Pore Sizes

Ville-Veikko Telkki, Juhani Lounila, and Jukka Jokisaari*

Department of Physical Sciences, NMR Research Group, University of Oulu, P.O. Box 3000, FIN-90014 University of Oulu, Finland

Received: July 20, 2004; In Final Form: October 26, 2004

^{129}Xe NMR spectra of xenon dissolved in acetonitrile confined into three mesoporous silica gels with nominal pore diameters of 40, 60, and 100 Å have been measured over the temperature range 170−245 K. The spectra consist of a number of lines, which contain detailed information on the system. The most interesting result is that the chemical shift of a particular signal observed below the melting point of confined acetonitrile is highly sensitive to the pore size, and hence its shape is sensitive to the pore size distribution function. This signal originates from the xenon atoms sited in very small cavities built up inside the pores during the freezing transition. It can be used to determine the size or even the size distribution function of the pores. In addition, the emergence of this signal reveals the phase transition temperature of acetonitrile inside the pores, which can also be used to determine the size of the pores. The difference in the chemical shifts of two other signals, which arise from xenon dissolved in bulk and confined acetonitrile, provides still another novel method for determining the size of the pores.

1. Introduction

Porous materials are solids with large internal surface, which mainly consist of walls of interconnected networks of pores and cavities. They are widely used in technological and scientific applications, and they have an important role in many natural processes. They are classified according to the pore size, and each class has its characteristic adsorption properties. *Mesoporous* materials, which have been studied in this project, are materials whose pore diameters are between 20 and 500 Å.[1]

The pore size distribution is one of the most important features of the materials, and reliable and efficient methods for its determination are of considerable interest. Pore sizes have classically been determined by a gas adsorption/desorption technique, mercury porosimetry, and thermoporosimetry.[2] However, these methods are quite time-consuming, and there have been efforts to develop novel methods. A significant one is NMR cryoporometry,[3−10] which has been an object of expanding interest during the latest decade. It is based on the observation of the melting point changes of a liquid confined to the pores. According to the Gibbs−Thompson equation,[11] the melting point depression ΔT is inversely proportional to the pore radius R_p:

$$\Delta T = T_0 - T = \frac{2\sigma_{sl}T_0}{\Delta H_f \rho_s R_p} \equiv \frac{k_p}{R_p} \qquad (1)$$

Here T_0 and T are the melting points of the bulk and confined liquid, respectively, σ_{sl} is the surface energy of the solid−liquid interface, ΔH_f is the specific bulk enthalpy of fusion, and ρ_s is the density of the solid. The constant k_p defined in eq 1 is specific to each probe liquid. In NMR cryoporometry, the amount of unfrozen fraction of the liquid is monitored as a function of temperature by the intensity of an ^{1}H NMR signal of the liquid. Thus the amount of the frozen or melted liquid at a certain temperature can be determined, and the pore size distribution can be calculated by the Gibbs−Thompson equation. One of the advantages of the NMR cryoporometry method is that it is nondestructive.

In the present study, the freezing and melting behavior of a confined liquid has been explored by means of the ^{129}Xe NMR resonance signals of xenon dissolved in the sample. Acetonitrile has been used as the probe liquid, and three different silica gels have been used as adsorbents. The chemical shift of xenon is known to be extremely sensitive to changes of its local environment. Therefore, one of the original aims of the project was to explore if it is possible to find a spectral component whose chemical shift is dependent on the pore size, thus obviating the arduous and inaccurate signal intensity measurements.

2. Experimental Section

Silica gels were delivered by Merck (Darmstadt, Germany). The nominal pore diameters of the materials are 40, 60, and 100 Å, and the sizes of the granules are between 63 and 200 μm. Hansen et al.[12] have recently determined the pore size distributions of these materials with three different methods (N_2 adsorption, ^{2}H NMR cryoporometry, and ^{2}H NMR spin−lattice relaxation times). The distributions are quite wide, but the average radii of the pores are close to the values announced by the manufacturer, and the tops of the distributions are well-defined. Hence, the materials are suited for model systems of mesoporous materials. Acetonitrile was obtained from Fluka (Buchs, Switzerland), and it was used without further purification after drying the liquid over molecular sieves.

The sample construction is shown in Figure 1. First, a xenon thermometer was set in the middle of an ordinary 10 mm thick wall sample tube propped by spacers. The thermometer is a capillary tube (diameter 2.7 mm) containing 1−2 cm of ethyl bromide in the bottom of the tube and about 1.5 atm of enriched xenon gas (70% of the atoms is ^{129}Xe). The ^{129}Xe chemical shift difference between the signals of xenon dissolved in ethyl

10.1021/jp046788f CCC: $30.25
Published on Web 12/24/2004

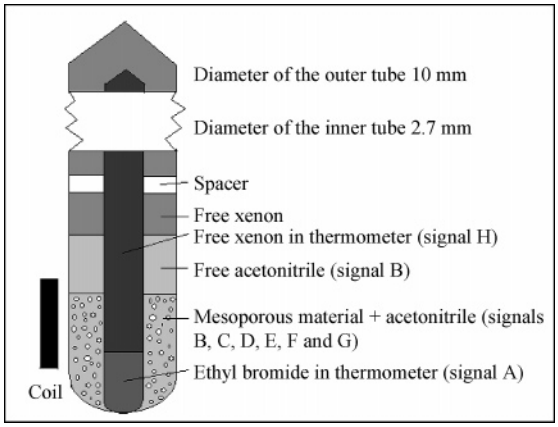

Figure 1. Sample tube construction.

bromide and bulk xenon gas is very sensitive to temperature, and the temperature was derived from the difference utilizing a calibration curve.[13] About 2.7 cm of silica gel powder was added to the annulus of the sample tube system, and the powder was dried by keeping the tube in a vacuum line overnight. After drying, acetonitrile was added so that a layer of bulk acetonitrile remained on top of the silica gel in the coil region of the spectrometer. The sample was degassed by first freezing it with liquid nitrogen and then thawing it out. Finally, about 3.4 atm of enriched xenon gas was added, and the glass tube was sealed with a flame.

One-dimensional ^{129}Xe NMR spectra were measured on a Bruker DRX500 spectrometer (resonance frequency 138.3 MHz). The spectra were recorded using a 10 mm high-resolution probehead over the temperature range 170−245 K applying 45° pulses (the length of the pulses was 13 μs), 7.8 s repetition time, and accumulating 200 scans. The steps of the temperature series were 2.5−5 K and the temperature was allowed to stabilize 20 min after each change. During an experiment, the monitored temperature varied less than ±0.1 K. The spectra were measured from low to high temperatures to avoid the supercooling effects of the liquid. The ^{129}Xe resonance signal measured at 230 K from a bulk xenon gas sample of pressure ∼6 atm (fixed to 0 ppm) was used as an external reference. Especially at the lowest temperatures, when wide signals occurred, the baseline of the spectra distorted and was manually corrected.

3. Assignment of the Signals

Figure 2 displays the ^{129}Xe NMR spectra of the sample containing silica gel 100 at different temperatures. The signals have been labeled in the figure (see also Figure 1), and the same spectral components are found from each sample. The origins of the components will be analyzed below.

Signal A. The sharp signal in the range 205−235 ppm, whose chemical shift vs temperature behavior is linear, originates from the xenon dissolved in ethyl bromide in the thermometer.

Signals B and C. Above 227 K, there are two signals, B and C, around 185 ppm. From this value of the chemical shift, it can be concluded that these signals arise from xenon dissolved in liquid acetonitrile. Signal B originates from the bulk acetonitrile, as it vanishes below the freezing temperature of this solvent (227 K). Indeed, spectra of a test sample containing only acetonitrile and xenon gas show that the signal of the dissolved xenon vanishes when acetonitrile freezes. A part of the signal B arises from dissolved xenon in the space between silica gel particles (diameter ∼ 100 μm). The other signal, C, gradually vanishes at much lower temperatures. An obvious

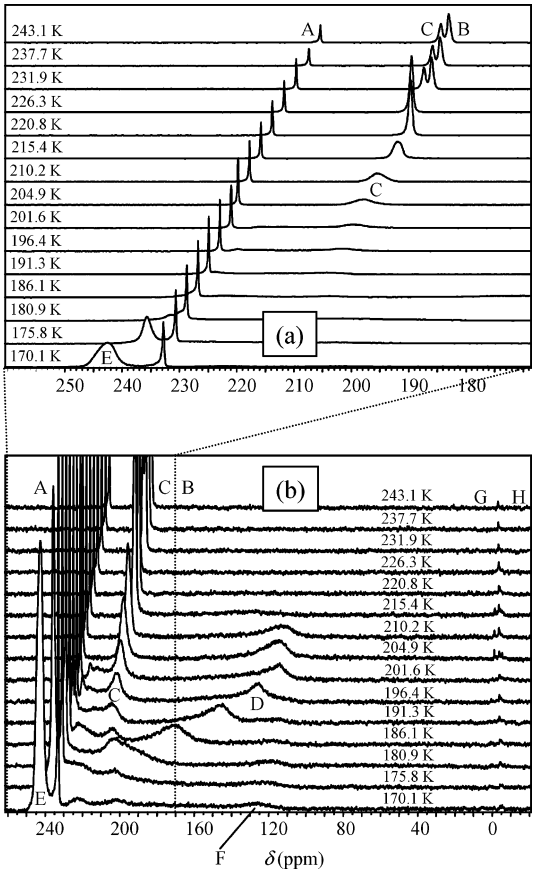

Figure 2. ^{129}Xe NMR spectra of the sample containing silica gel 100 at different temperatures: (a) expanded chemical shift (δ) range of the signals A−C and E; (b) chemical shift range of all the signals. The intensities of the spectra have been amplified so that the components D and F−H are distinguished better. The measurement temperatures are shown between the spectra.

interpretation is that this signal arises from xenon dissolved in liquid acetonitrile *confined to the pores*. The slightly higher chemical shift of signal C, compared with that of signal B, is due to the interaction of the xenon atoms with the surface of the pores. Below the melting point of the bulk acetonitrile, the pores freeze gradually from the biggest to smallest ones with lowering temperature, and the intensity of signal C decreases. During the freezing of the bulk acetonitrile, the intensity of signal C is seen to increase abruptly. This is probably due to the fact that a part of the xenon that is released from the frozen bulk acetonitrile ends up into the liquid acetonitrile inside the pores.

Signal D. In the cases of silica gel 100, 60, and 40, signal D emerges below 216, 209, and 205 K, respectively. It is strongly and nonlinearly temperature dependent. The most prominent feature of signal D is its location between the signals of xenon dissolved in liquid bulk acetonitrile (signal B) and xenon gas in free space (close to 0 ppm). The only conceivable explanation for this intermediate value of the chemical shift is that the local surroundings of the respective xenon atoms are, on the average, somewhat less dense than in liquid acetonitrile. As explained in detail in the next section, a plausible interpretation is that signal D arises from the xenon atoms sited in very small cavities built up inside the pores of the silica gels. At lower temperatures, there is rapid exchange of xenon atoms between the liquid and gas phase, which accounts for the striking temperature dependence of the signal.

Signal E. The signal is seen at the lowest temperatures, below 180 K. From its high chemical shift, around 240 ppm, it can be

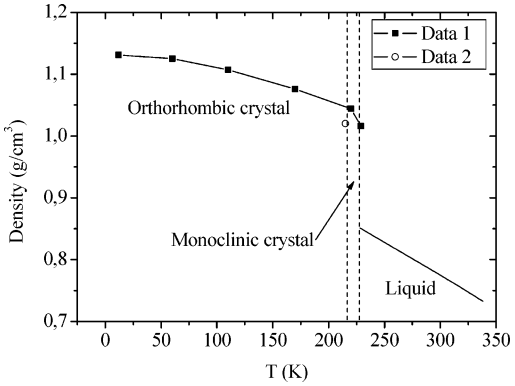

Figure 3. Density and phases of acetonitrile as a function of temperature. Data 1 have been calculated by means of the crystal structures determined by Torrie et al.[16] The solid lines between the symbols are to guide the eye. Point 2 was published by Barrow[17] and the phase of the measurement was monoclinic. The liquid density curve has been taken from ref 18. The solid−solid phase transition temperature was measured by Putman et al.[19]

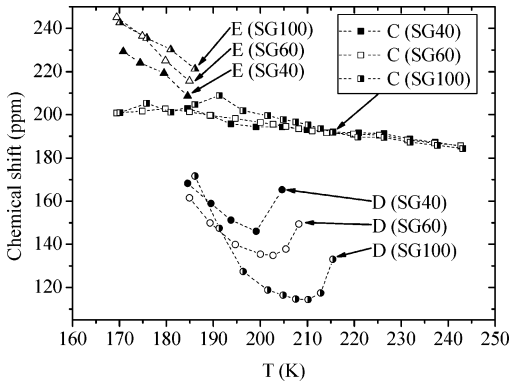

Figure 4. Chemical shifts of signals C−E as a function of temperature in the case of different silica gels (abbreviated SG). The filled symbols belong to silica gel 40, the open symbols to silica gel 60, and the half filled to silica gel 100. The dashed lines between the symbols are to guide the eye. The low-temperature data points of signal D have been omitted from the figure as the chemical shift determination is inaccurate due to the overlap of the signals.

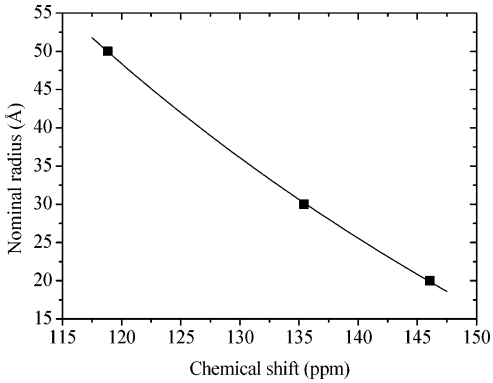

Figure 5. Nominal radius R_p with respect to the chemical shift of signal D at 200 K.

deduced that it arises from the liquefied xenon (xenon liquefies at 180 K, if its pressure is 2 atm[14]).

Signal F. In the case of silica gel 100 (but not for the other silica gels), there is at low temperatures a very weak signal around 120 ppm. It differs from signal D in that its temperature dependence is weak and linear. These characteristics imply that signal F arises, as signal D, from the small cavities built up inside the pores, but from *gaseous* xenon only, *without the gas−liquid exchange*. As this occurs only in the largest cavities, a conceivable reason is that there are regions in these cavities where the exchange is so slow that separate signals are observed for gaseous and liquid xenon.

Signals G and H. The two weak signals around 0 ppm arise from gaseous xenon either in the cavities within solid bulk acetonitrile (G) or in the capillary tube of the thermometer (H). The cavities are formed when the bulk acetonitrile freezes between the silica gel particles. They are so large that no exchange effects are observable and the chemical shift of xenon is close to that of free xenon. The intensity of the signals G and H is low due to partial saturation of signals, as the repetition time of the measurements (7.8 s) was short compared to the long T_1 relaxation time of gaseous xenon (even above 3 h in the case of bulk gas[15]). At low temperatures, the liquefaction of xenon leads to a further decrease in the intensity of the signals.

4. Analysis

4.1. Origin of Signal D. The density of bulk acetonitrile increases rapidly with decreasing temperature, as can be seen from Figure 3. At the freezing point (227 K), the density increases abruptly about 20%. Thus, if liquid acetonitrile fills a closed and rigid container, empty voids of about 17% of the total volume of the container are built up inside it upon freezing. This is what happens to acetonitrile confined to the pores of the silica gels, as the surrounding bulk acetonitrile has frozen earlier and cannot enter the pores. Evidently, the volume of the void formed in a pore is directly proportional to the volume of the pore.

On the other hand, a transition from liquid to solid is generally accompanied by an abrupt reduction of gas solubility. Therefore, the xenon gas dissolved in liquid acetonitrile is expected to be released, to a great extent, from the solvent during solidification. If this happens inside a closed pore, xenon ends up into the empty void grown in the pore. Hence immediately below the freezing temperature of the confined acetonitrile, the pore contains solid acetonitrile and a pocket filled by xenon gas. Signal D is expected to arise from these pockets. The pockets may be inside the solid acetonitrile or between the solid acetonitrile and the walls of the pores. However, it has been shown that there exists a layer of nonfrozen liquid at the pore wall[20] so that it is reasonable to assume that the pockets are always completely surrounded by acetonitrile, and xenon gas inside the pocket does not directly interact with the surface of the pore.

The perturbation due to the interaction of a xenon atom with its surroundings lowers the magnetic shielding of the xenon nucleus, σ. The smaller the gas pocket is, the stronger the perturbation is, and the higher the chemical shift $\delta = \sigma_{ref} - \sigma$ of the xenon atoms is. Because the size of the pocket is directly proportional to the size of the pore, the chemical shift of signal D is expected to decrease with increasing pore size. This prediction is in agreement with the experimental data, as can be seen from Figure 4. In fact, this dependence can be used to determine the size of the pore. Figure 5 shows that in the restricted range of the nominal pore radii $R_p = 20$, 30, and 50 Å at 200 K the dependence of R_p on δ can be approximated by the simple model function

$$R_p = \frac{a}{\delta} - b \qquad (2)$$

TABLE 1: Pore Radii of the Silica Gels, R_P, Calculated by the Gibbs−Thompson Equation

material	T (K)	ΔT (K)	R_p (Å)	R_{cryo}
silica gel 40	204.6	22.4	24	24.3
silica gel 60	208.2	18.8	29	27.1
silica gel 100	215.4	11.6	47	45.5

[a] Here, T is the highest temperature at which signal D is observable, $\Delta T = T_0 - T$, where $T_0 = 227$ K is the melting point of bulk acetonitrile, and $R_p = k_p/\Delta T$, where the constant $k_p = 545$ K Å has been measured by Aksnes et al.[9] For comparison, the average pore radii of the materials measured by NMR cryoporometry method, R_{cryo}, are shown in the table.

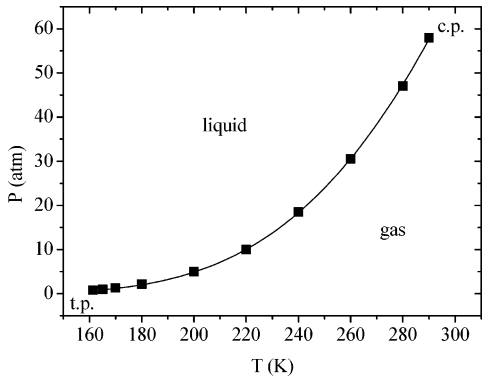

Figure 6. Vapor pressure of xenon as a function of temperature and fitted Clausius−Clapeyron curve.[14,21] Abbreviations t.p. and c.p. denote triple and critical points, respectively.

which exhibits correct asymptotic behavior at the limits of small and large pores. A least-squares adjustment of the parameters a and b resulted in the values $a = 19171$ Å/ppm and $b = 111.4$ Å.

According to the above interpretation, signal D emerges during the solidification of acetonitrile confined to the pores. Thus the emergence or disappearance of signal D reveals the phase transition temperature inside the pores. This, together with the Gibbs−Thomson equation (eq 1), provides another novel method for determining the size of the pores. This is demonstrated in Table 1, which shows the highest temperatures at which signal D can be seen in silica gel 40, 60, and 100, T, the corresponding melting point depressions $\Delta T = T_0 - T$, where $T_0 = 227$ K, and the pore radii calculated by $R_p = k_p/\Delta T$, where the coefficient $k_p = 545$ K Å has been determined by Aksnes et al.[9] The resulting values of R_p are very close to the nominal pore radii $R_p = 20$, 30, and 50 Å, in view of the uncertainty in the temperature at which signal D emerges. As explained in more detail in the next section, the signal comes into view gradually, which may reflect the fact that the cavities grow up or shrink down gradually during the freezing or melting of acetonitrile, respectively. For comparison, the average pore radii of the materials (R_{cryo}) were determined by the NMR cryoporometry method by measuring ^{1}H NMR spectra over a wide temperature range from all the samples, and analyzing the ^{1}H intensities as Aksnes describes.[9] The results are presented in Table 1, and they are in very good agreement with the values extracted from ^{129}Xe spectra.

4.2. Temperature Dependence of Signal D. Values of the vapor pressure of xenon as a function of temperature have been plotted in Figure 6.[14] The vapor pressure curve can be approximated by the Clausius−Clapeyron equation[21]

$$P = A \exp\left(-\frac{l}{RT}\right) \tag{3}$$

where A is a constant, l is the molal heat of vaporization, R is the universal gas constant, and T is temperature. A least-squares adjustment of the parameters A and l resulted in the values $A = 14\,012$ atm and $l = 13\,244$ J/mol. The latter value is quite close to the measured value of the heat of vaporization at the boiling point (at ambient pressure), 12 640 J/K.[22]

Consider a small closed cavity of fixed volume V containing n moles of a substance. At a temperature T above or below the boiling point T_b, the vapor pressure can be approximated by the ideal gas equation $P = nRT/V$ or by the modified Clausius−Clapeyron equation

$$P = \frac{nRT_b}{V} \exp\left[\frac{l}{R}\left(\frac{1}{T_b} - \frac{1}{T}\right)\right] \tag{4}$$

respectively. Hence, below T_b, the fraction of the substance in the gas phase is

$$p_g = \frac{PV}{nRT} = \frac{T_b}{T} \exp\left[\frac{l}{R}\left(\frac{1}{T_b} - \frac{1}{T}\right)\right] \tag{5}$$

and the rest, fraction $p_l = 1 - p_g$, is in the liquid phase. If the cavity is very small, there is fast exchange of the molecules between the two phases, and the observed chemical shift of a particular nucleus is the weighted average

$$\delta = p_g\delta_g + p_l\delta_l = \delta_l - (\delta_l - \delta_g)\frac{T_b}{T} \exp\left[\frac{l}{R}\left(\frac{1}{T_b} - \frac{1}{T}\right)\right] \tag{6}$$

where δ_g and δ_l are the chemical shifts in the gas and liquid phase, respectively.

In Figure 7, the chemical shifts of signals C−E have been plotted as a function of temperature and the graphs have been divided into three different regions, I−III:

(I) This is the region below the boiling point (T_b) of xenon, where T_b is slightly less than 200 K at the pressures of the present samples. In this region eq 6 is valid, and it has been fitted to the data points of signal D by least-squares adjustment of the parameters.

(II) This is the region above the boiling temperature of xenon but below the point T_s where the melting of confined acetonitrile begins (around 200 K). In this region, the chemical shift of signal D changes mainly due to exchange of xenon gas between different sites. Two-site exchange models such as those used to explain the behavior of pure xenon gas in microporous materials[23−25] have been tested to the data points and have been found to account for the changes of the chemical shifts with realistic parameter values. However, because the region is very narrow, the resulting values are inaccurate, and therefore such fits are not presented here. Instead, straight lines have been fitted to the data points of signal D.

(III) This is the region of width 4−5 K above the temperature T_s where signal D gradually fades away during the melting of confined acetonitrile. A rapid decrease in the intensity of the signal with increasing temperature is accompanied by a sharp rise of its chemical shift. It is conceivable that the gas pockets inside the pores shrink down gradually during the melting of acetonitrile. As the volume of acetonitrile increases, the pockets become smaller, and the chemical shift of xenon gas inside them increases, finally approaching that of xenon dissolved in liquid acetonitrile. Also in this region the changes of chemical shifts have been depicted by straight lines. These lines continue (as dashed lines) to the chemical shifts of xenon dissolved in unfrozen acetonitrile in the pores. The values of the parameters obtained from the fits have been listed in Tables 2 and 3.

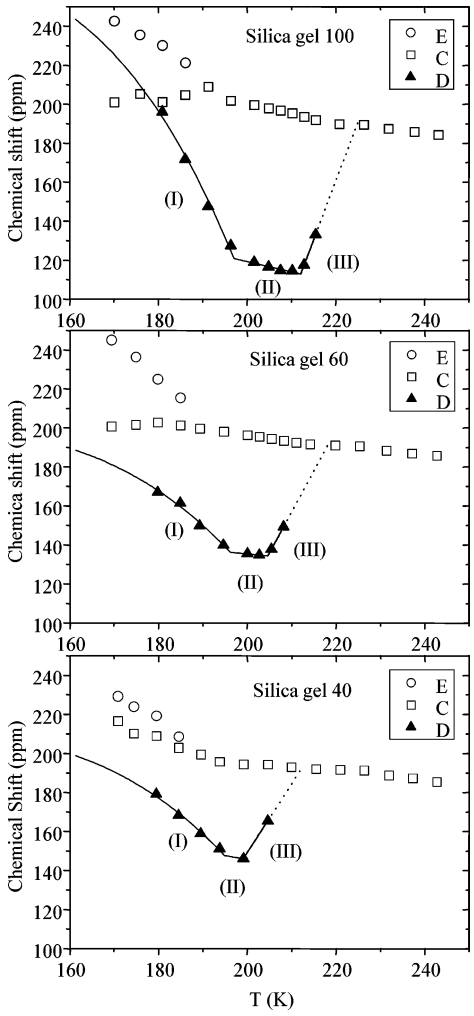

Figure 7. Chemical shifts of signals C−E as a function of temperature and fits of the data points of signal D in the case of different silica gels. In region I, there is rapid exchange of xenon atoms between liquid and gas phase. In region II (between temperatures T_b and T_s), signal D arises from gaseous xenon only. In region III, the confined acetonitrile solvent is gradually melting.

TABLE 2: Parameters Resulting from the Fittings of Eq 6 to the Data Points of Signal D in Region I

material	T_b (K)	δ_g (ppm)	δ_l (ppm)
silica gel 40	194.8	147.7	213.3
silica gel 60	196.1	136.3	202.4
silica gel 100	197.1	120.9	274.9

[a] The molal heat of vaporization, *l*, has been kept fixed to the value of 13 244 J/mol obtained in fitting the Clausius−Clapeyron equation (eq 3) to the vapor pressures.

TABLE 3: Parameters Resulting from the Fittings of the Straight Lines $\delta = x + yT$ to the Data Points of Signal D in Regions II and III

	region II		region III		
material	x (ppm)	y (ppm/K)	x (ppm)	y (ppm/K)	T_s (K)
silica gel 40	221.0	−0.3764	−556.5	3.5277	199.1
silica gel 60	179.7	−0.2213	−722.5	4.188	204.6
silica gel 100	225.6	−0.5315	−1169	6.044	212.1

According to Table 2, the boiling point of xenon in the pockets, T_b, is nearly constant, about 196 K. From the vapor pressure curve (eq 3), the corresponding pressure of xenon vapor is about 4.1 atm. At this temperature, the xenon gas pressure in a sample tube assumed to be empty has been calculated to be about 2.3 atm. This seems reasonable, because the part of the xenon gas dissolved in liquid acetonitrile is largely accumulated from the solvent to the pockets during solidification, increasing its pressure. On the other hand, the liquefaction of gas in the small pocket may begin at lower pressures than that of bulk gas due to capillary condensation.[26]

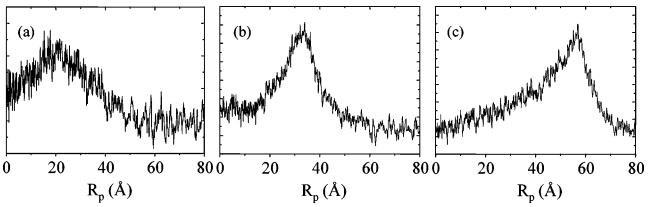

Figure 8. Pore size distributions of (a) silica gel 40, (b) silica gel 60, and (c) silica gel 100 depicted by means of the shape of signal D measured at 200 K and the relation between R_p and δ, eq 2.

Also the resulting values of the chemical shifts δ_g and δ_l seem realistic. Terskikh et al.[27] have determined a general correlation for the ^{129}Xe chemical shift−pore size relation in porous silica-based materials over the range 5−400 Å in diameter. Unfortunately, the correlation cannot be used for estimation of pocket sizes, as the measurement temperatures and the gas pressures differ. However, we have measured ^{129}Xe spectra over a wide temperature range from the sample containing silica gel 40 and about 4 atm of xenon gas, and at 200 K, the chemical shift of xenon inside the pores is 100.6 ppm. Because the volume of the pocket is approximately 17% of the volume of the pore, the 47 ppm higher δ_g value measured from the pockets is reasonable. As expected, the smaller the pore (and hence the gas pocket) is, the higher the chemical shift of the xenon atoms is. There is large scatter in the values of δ_l, but their average value, 230 ppm, is close to the chemical shift of liquefied xenon, as it should be.

In the case of silica gel 40, region II is very narrow and contains only one data point. Therefore, the slope of the straight line depicting this region, *y*, was constrained to the average value of the corresponding slopes for silica gel 60 and 100.

4.3. Pore Size Distribution from the Shape of Signal D. Preceding results show that there is one-to-one correspondence, such as relation 2, between the pore size and the chemical shift of signal D measured at some particular temperature. In consequence, a *distribution* of pores of different sizes produces a corresponding distribution of signals of different chemical shifts, i.e., a characteristic NMR line shape. Thus it may be possible to extract the pore size distribution function from the shape of signal D. This can be done simply by converting the chemical shift scale of the NMR spectrum to the pore size scale by eq 2, provided that the intrinsic line width of signal D arising from approximately spherical gas pockets is small in comparison with the line width resulting from the pore size distribution. This also presumes that the density of xenon is independent of the pocket size, and there is no saturation of the signal. Then the intensity of the signal at a particular chemical shift is directly proportional to the total volume of the pores of the corresponding size. The pore size distributions of silica gels obtained by this simple method, using eq 2, have been plotted in Figure 8.

Not surprisingly, the centers of mass of the distributions coincide with the nominal pore sizes, as the same signals have been used to calibrate the relation between the pore size and the chemical shift. Although the maxima are well-defined, the resulting distributions are rather broad—the full width at half-maximum of all the distributions is of the order of 20 Å. The results are in agreement with the distributions determined by NMR cryoporometry and N_2 adsorption.[12]

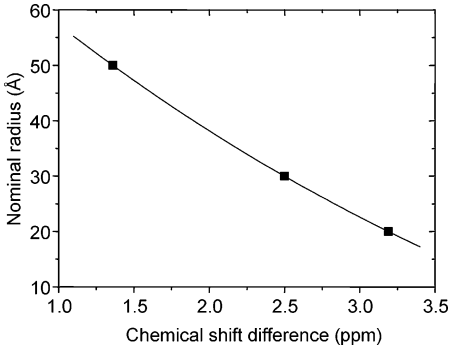

Figure 9. Nominal radius R_p as a function of the difference of the chemical shifts of signals C and B at 230 K.

4.4. Difference in the Chemical Shifts of Signals B and C. Signals B and C arise from xenon dissolved in bulk and confined acetonitrile, respectively. Consequently, the difference in their chemical shifts, $\delta_C - \delta_B = \Delta\delta$, is expected to decrease with increasing pore size. This prediction is in agreement with the experimental data, as can be seen from Figure 9. Several functional forms were tested for the model function of the relation between $\Delta\delta$ and R_p, the nominal radius of the pore, and finally the expression

$$R_p = c \exp\left(-\frac{\Delta\delta}{d}\right) - f \tag{7}$$

was chosen. A least-squares refinement of the parameters c, d, and f resulted in the values $c = 126.0$ Å, $d = 4.83$ ppm, and $f = 46.1$ Å at 230 K (immediately above the melting point of bulk acetonitrile).

In principle, this relation provides a very convenient method for determining the size of the pores. Because the chemical shifts of both signals are linear functions of temperature, it is straightforward to use the relation at any temperature above the melting point of acetonitrile. However, the method is not very accurate, because $\Delta\delta$ (of the order of a few ppms) is not much larger than the line widths of the signals B and C (about one ppm), at least when acetonitrile is used as a solvent.

5. Conclusions

The present study demonstrates that ^{129}Xe NMR of xenon dissolved in acetonitrile confined into mesoporous materials can give detailed information on the system. The most interesting signal arises from the xenon atoms sited in very small cavities built up inside the pores during the freezing transition. It provides a novel method for determining the size of the pores, because the chemical shift of this signal is highly sensitive to the pore size, and the shape of the signal depicts the pore size distribution. Moreover, the emergence or disappearance of the signal reveals the phase transition temperature of acetonitrile inside the pores. This, together with the Gibbs−Thomson equation, can be used to determine the sizes of the pores. Another conspicuous signal originates from xenon dissolved in liquid acetonitrile confined to the pores. Because of the interactions with the surface of the pores, the chemical shift of this signal is slightly higher than that of the signal from the bulk acetonitrile. Therefore, the difference in the chemical shifts of these two signals can also be used to determine the pore sizes.

The chemical shift of pure xenon gas in a mesoporous material (without any solvent) is also dependent on the pore size.[27] However, ^{129}Xe NMR spectra of such samples are not as rich as the spectra obtained in the present study. Hence the use of a liquid solvent such as acetonitrile increases the information content of the spectra. Another possible advantage of using a solvent pertains to the mechanism of the environmental effect on xenon. If the xenon atoms interact directly with the surfaces of the pores, the effect on the chemical shift is sensitive to the specific properties of the surface material. Therefore, the relation between the chemical shift and pore size may be highly specific to the material. However, if the xenon atoms interact mainly with the solvent molecules, then this relation can be expected to have more universal validity. This means that the chemical shift of xenon in different porous materials filled with the same solvent such as acetonitrile is expected to exhibit approximately similar behavior, irrespective of the nature of the material. Perhaps the most important advantage relates to the pore size distribution. In the case of pure xenon gas in mesoporous materials, the xenon atom has time to visit in several pores of different sizes during an NMR measurement, and the observed chemical shift is the weighted average of the chemical shifts characteristic of these pore sizes. However, when the system contains also solvent, and the temperature is below the melting point of the confined solvent, the xenon atom in the pore has been closed off inside the pocket formed by solid solvent, and the walls of the pocket prevent the atom to move from one pore to another. Thus, the observed resonance frequency exactly corresponds to the one particular pore size. The distribution of the resonance frequencies obtained from xenon atoms in different pockets (signal D) directly represents the pore size distribution.

The method introduced in this article makes it possible to measure the pore sizes of mesoporous materials by three novel means. In addition, it is also possible to determine the pore size distribution by a single measurement at constant temperature. Usually, the term porosimetry refers to methods for measuring porosity (which is the ratio of the volume of voids to the total volume of the porous material) whereas the term porometry refers to methods for determining the pore dimensions such as the pore size and pore size distribution, although occasionally in the literature the difference of these concepts is not clear. Therefore, we propose, that the present method may be referred to as xenon porometry.

References and Notes

(1) Webb, P. A.; Orr, C. *Analytical Methods in Fine Particle Technology*; Micrometrics Instrument Corp.: Norcross, GA, 1997.

(2) Dullien, F. A. L. *Porous media: Fluid Transport and pore Structure*, 2nd ed.; Academic Press: San Diego, 1992.

(3) Overloop, K.; Van Gerven, L. *J. Magn. Reson. A* **1993**, *101*, 179.

(4) Strange, J. H.; Rahman, M. *Phys. Rev. Lett.* **1993**, *71*, 3589.

(5) Hansen, E. W.; Schmidt, R.; Stöcker, M. *J. Phys. Chem.* **1996**, *100*, 11396.

(6) Schmidt, R.; Hansen, E. W.; Stöcker, M.; Akporiaye, D.; Ellestad, O. H. *J. Am. Chem. Soc*. **1995**, *117*, 4049.

(7) Hansen, E. W.; Stöcker, M.; Schmidt, R. *J. Phys. Chem*. **1996**, *100*, 2195.

(8) Morishige, K.; Kawano, K. *J. Chem. Phys.* **1998**, *110*, 4867.

(9) Aksnes, D. W.; Førland, K.; Kimtys, L. *Phys. Chem. Chem. Phys*. **2001**, *3*, 3203.

(10) Aksnes, D. W.; Førland, K.; Kimtys, L.; Stöcker, M. *Appl. Magn. Reson*. **2001**, *20*, 507.

(11) Jackson, C. L.; McKenna, G. B. *J. Chem. Phys.* **1990**, *93*, 9002.

(12) Hansen, E. W.; Simon, C.; Haugsrud, R.; Raeder, H.; Bredesen, R. *J. Phys. Chem. B* **2002**, *106*, 12396.

(13) Saunavaara, J.; Jokisaari, J. To be published.

(14) Cook, G. A. *Argon, Helium and Rare Gases*; Interscience Publishers: New York, 1961.

(15) Ratcliffe, C. I. *Annu. Rep. NMR Spectrosc.* **1998**, *36*, 124.

(16) Torrie, B. H.; Powell, B. M. *Mol. Phys.* **1992**, *75*, 613.

(17) Barrow, M. J. *Acta Crystallogr., Sect. B* **1981**, *37*, 2239.

(18) West, C. J.; Dorsey, N. E. *International Critical Tables of Numerical Data*: *Physics, Chemistry and Technology*; McGraw-Hill Book Co.: New York, 1928.

(19) Putman, W. E.; McEachern, D. M.; Kilpatrick, J. E. *J. Chem. Phys*. **1965**, *42*, 746.

(20) Valiullin, R., Furó, I. *J. Chem. Phys.* **2002**, *117*, 2307.

(21) Sears, F. W.; Salinger, G. L. *Thermodynamics, Kinetic Theory and Statistical Thermodynamics*; Addison-Wesley Publishing Co.: Reading, MA, 1976.

(22) Weast, R. C. *CRC Handbook of Chemistry and Physics 1983*−*1984*; CRC Press: Boca Raton, FL, 1985.

(23) Chen, Q. J.; Fraissard, J. *J. Phys. Chem*. **1992**, *96*, 1809.

(24) Raftery, D.; Reven, L.; Long, H.; Pines, A.; Tang, P.; Reimer, J. A. *J. Phys. Chem*. **1993**, *97*, 1649.

(25) Koskela, T.; Ylihautala, M.; Jokisaari, J. *Microporous Mesoporous Mater*. **2001**, *46*, 99.

(26) Wilkinson, N. J.; Alam, M. A.; Clayton, J. M.; Evans, R.; Fretwell, H. M.; Usmar, S. G. *Phys. Rev. Lett.* **1992**, *69*, 3535.

(27) Terskikh, V. V.; Moudrakovski, I. L.; Breeze, S. R.; Lang, S.; Ratcliffe, C. I.; Ripmeester, J. A.; Sayari, A. *Langmuir* **2002**, *18*, 5653.